6th AIAA Flow Control Conference
25 - 28 June 2012, New Orleans, Louisiana

AIAA 2012-2951

Experimental Studies of DBD Actuator Effects on Wing Tip Vortex Topology

A. Leroy[1]
PRISME, University of Orléans, 45072 Orléans Cedex 2, France

P. Molton[2] *and* Y. Carpels[3]
ONERA, 8 rue des Vertugadins, 92190 Meudon, France

and

J. Pons[4]
EPEE, CNRS / University of Orléans, 45067 Orléans Cedex 2, France

Experiments studying the wing tip vortex, generated by a rectangular wing with a symmetric airfoil section and a straight tip, manipulated by surface plasma actuators are presented in this paper. Objectives are focused on modifying vortex development to alter streamwise vorticity downstream of the wing trailing edge. Actual limitation of the ionic wind magnitude obtained with DBD actuators leads to investigate vortex control by action on the transverse component of the freestream flow velocity. Different DBD arrangements installed near the wing tip were tested to examine effects of momentum addition, firstly on the pressure and suction side surfaces, and secondly, simultaneously located more precisely on the main vortex separation and attachment lines. Stereoscopic PIV measurements were performed in different planes orthogonal to the vortex development axis to visualize and characterize wing tip vortices. According to DBD arrangements, results of the actuation show a slight displacement of the wing tip vortex and a reduction of the mean streamwise vorticity level in its core.

Nomenclature

c	=	chord
U_0	=	freestream velocity
X	=	chord axis
Y	=	transverse axis
Z	=	vertical axis
U	=	chord axis velocity
V	=	transverse axis velocity
W	=	vertical axis velocity
k	=	turbulent kinetic energy
Ω_x	=	streamwise vorticity

I. Introduction

Reduction of wing tip vortices generated by an aircraft wing is of importance in practical engineering issues, such as saving fuel consumption and minimizing aircraft separation time during takeoff. On helicopter blades and propellers, tip vortices cause rotor noise and vibration[1-4]. For these reasons many studies focusing on reducing

[1] Associate Professor, PRISME, 8 rue Léonard de Vinci, 45072 Orléans cedex 2, France, AIAA Member.
[2] Research Engineer DAFE, ONERA, 8 rue des Vertugadins, 92190 Meudon, France, AIAA Member.
[3] Senior Technician, DAFE, ONERA, 8 rue des Vertugadins, 92190 Meudon, France.
[4] Post-doctoral fellow, EPEE, CNRS / University of Orléans, BP 6744, 45067 Orléans Cedex 2, France.

their vorticity have been conducted during the last decades[5]. Passive control techniques like winglets and active control techniques such as mobile flaps, suction or blowing devices[6] have been used to reduce tip vortices. Corke et al[7] provided an overview of main capabilities of active control by surface Dielectric Barrier Discharge (DBD) actuators, discussing the optimization of design, placement and operation mode. Up to now, most applications of DBD actuators dedicated to flow control have focused on modifying the longitudinal component of the flow velocity by momentum addition in steady or burst mode. Investigations on modifying the transverse component of the flow velocity seem necessary to achieve a modification of wing tip vortices. The possibility of vortex flow control by DBD actuators on a delta-wing model was studied at high angles of attack and subsonic speed[8]. It was demonstrated that DBD actuators can be successfully applied to modify the vortex breakdown location but also to stabilize vortex when operating in burst mode. Plasma actuation on the wing tip vortex of rectangular wing[9-11] has been investigated experimentally and numerically and has shown different influences of the actuation on the wing tip vortex formation according to a suction or blowing effect produced by actuators. Results on aerodynamic performance modification, lift increase[8] for example, differ with the study cases. More investigation is still necessary to find out optimized DBD arrangements.

According to the wing tip vortex topology[12,13] and to results[14] showing that particular steady blowing configurations near the wing tip are effective, this present study aims at experimentally investigating DBD actuator devices for modifying the wing tip vortex of a rectangular wing placed with a straight tip at an incidence of 6° in a freestream flow of 10 m/s. Main objectives are to demonstrate actuator potentialities to modify the development, position and strength of these vortices, as well as to alter streamwise vorticity downstream of the wing trailing edge, by acting on the transversal component of the flow velocity. Various DBD actuator arrangements were then implemented near the wing tip along the chord to generate a body-force field that couples with the momentum in the transverse direction of the main freestream flow. Flow investigation through the use of stereoscopic Particle Imaging Velocimetry (PIV) was performed to visualize and characterize wing tip vortices following planes orthogonal to the vortex development axis, on the wing and in the near wake. Control effectiveness while increasing the velocity of the freestream flow was also tested. After a presentation of the global experimental setup and actuator arrangements, results on the mean streamwise vorticity and turbulent kinetic energy are discussed according to DBD arrangements to highlight effects of this active control.

II. Experimental setup

A. Model and topology of the wing tip vortex

The tests were conducted in the F2 wind tunnel at the ONERA Fauga-Mauzac center, which is an atmospheric wind tunnel with a return circuit. The convergent has a contraction ratio of 12:1. The test section is 5-m-long, and has a 1.4-m-wide and 1.8-m-high rectangular cross section. It is equipped with glass and wood interchangeable walls. The maximum freestream velocity is 100 m/s. The model consists in a rectangular wing having a symmetric profile (AFV82), a straight tip with sharp edges, a span equal to 1050 mm and a chord equal to 300 mm (Fig. 1). The angle of attack was set at 6° and main tests were performed at 10 m/s corresponding to a Reynolds number of 2 x 10^5. A removable part for the wing tip was manufactured in order to implement actuators to be tested.

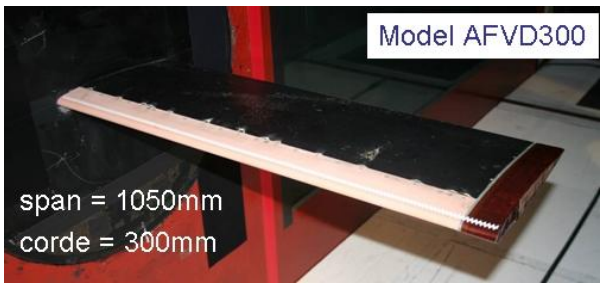

Figure 1. Rectangular wing in the test section.

B. Baseline flow topology of the wing tip vortex

Aerodynamic characteristics of the flow to be controlled have been studied at ONERA in previous work. Thus, measurements by three-component LDV (Laser Doppler Velocimetry) were performed in three planes located on the upper surface of the airfoil at positions along the non-dimensional chord direction (see Fig. 3): X/c = -0.5, -0.25, and -0.1. Results are presented in terms of iso-values of mean streamwise vorticity and velocity vectors in these planes in Fig. 2. They show that flow topology consists of a double vortex system at X/c =-0.5, the first one between the lower side of the model and the end of the tip, and the second one, between this end and the upper side. Further along the chord, they interact together and a main large vortex is formed on the suction side. Indeed, this flow

complexity indicates that the action of a single actuator system will be insufficient to control the vortex downstream of the model.

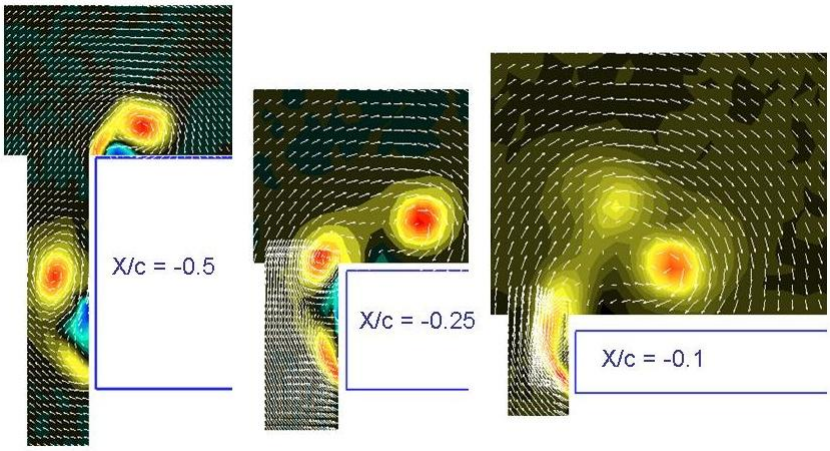

Figure 2. Natural flow topology of the wing tip vortex.

C. Stereo-PIV system in the F2 wind tunnel

For this study 3C-PIV (stereoscopic PIV) measurements were performed to visualize and characterize vortices. The wind tunnel is equipped with a three-component PIV system mounted on a mobile frame, which can carry out explorations along the entire length of the test section (Fig. 3). Three plans have been selected at the following positions along the non-dimensional chord direction: X/c = -0.25, 0.05, and 0.5 as shown in Fig. 3. The experimental process consisted, for each test case, to measure the natural flow field (case Off) with the actuators mounted on the wing to consider the influence of possible geometry changes, and to measure the modified flow field (case On) performed with the actuation.

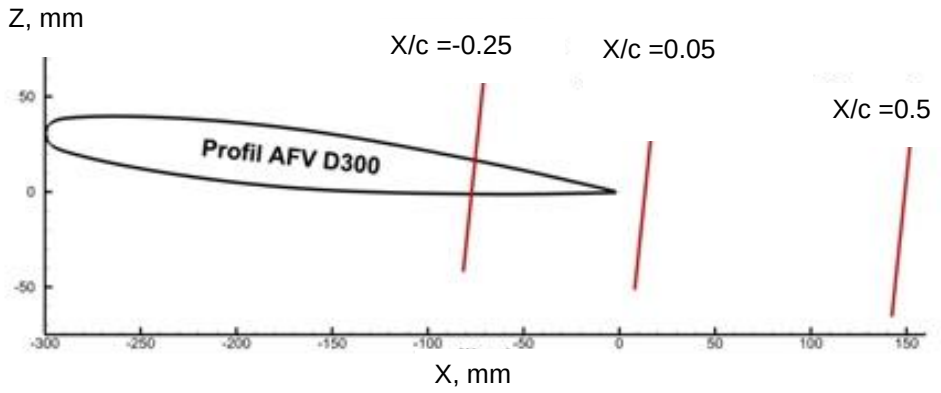

Figure 3. Position of the stereo-PIV planes: X: chord axis, Z: vertical axis.

The PIV system consists of a pulsed 2x400 mJ Nd/YAG laser, with a wavelength λ = 532 nm. The acquisition of the image pairs is performed by two PCO Imagerpro X4M-G (2048x2048 pixels, 1 pixel = 4.4 µm x 7.4 µm) cameras. Each camera is equipped with a motorized Scheimplug system, an auto-focus controller, a 135mm Nikon lens and an interference filter of wavelength λ = 532 nm. As shown in Fig. 4, PIV cameras and laser device are located on a system of displacement along the three axes X, Y, and Z, allowing reproducible positions of the measurement planes. The flow is seeded with oil droplets emitted by a device implanted at the inlet of the diffuser downstream of the test section. The average size of the droplets is of the order of 1µm. Management of image acquisition is performed by the Davis software 7.2. The laser pulse rate is set at 5Hz, and the time between two

images depends on the velocity of the freestream flow (between 15 and 30 μs). Image processing is performed using the ONERA PIV software FOLKI[15,16]. This software, optimized for massively parallel architectures like Graphics Processing Units (GPUs), produces dense vector fields with very limited computing cost. Moreover, for each configuration, a mask is suitable for avoiding calculating vectors in the model, and hiding areas dazzled by the reflections of the laser plane. Statistics on the flow are calculated based on 500 or 1000 instantaneous snapshots.

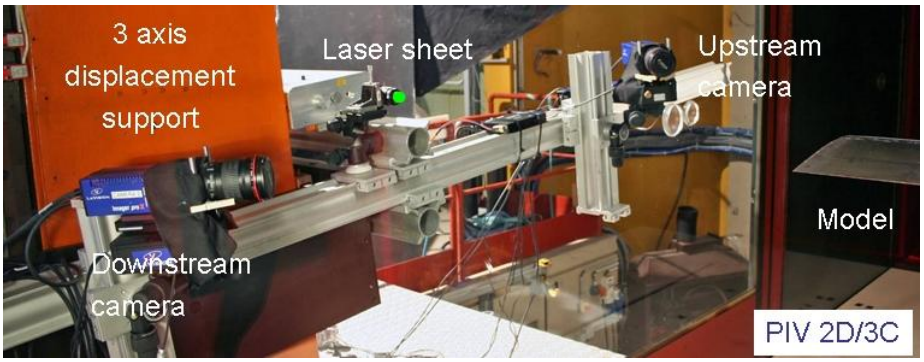

Figure 4. Stereo-PIV system in the F2 wind tunnel.

III. Actuator arrangements

Two different sets of DBD arrangements on the wing tip were investigated to search for the most effective decrease of the vortex strength. They were tested in two successive series of tests. For each set, DBD actuators were implemented around the wing tip at the same time but were operated either separately or simultaneously.

The first eight arrangements, presented in Fig. 5, consisted of surface DBD actuators located along the chord on the suction and pressure sides near the wing tip. In DBDs 1-4 one single DBD is operated whereas in DBDs 5-8 two DBDs are simultaneously operated. Depending on the ground and active electrode position, the ionic wind produced by DBDs has a different direction indicated by an arrow in the corresponding schemes. Main objective of the actuation is to interact with the separation of both shear layers emitted at the lower and upper sharp edges in order to modify the vortex formation and development. These DBD actuators consisted of two flush-mounted copper electrodes arranged asymmetrically on both sides of a dielectric composed of 0.3-mm-thick Mylar covered with two 0.05-mm-thick polyimide layers. The wing tip model was manufactured in order to insert actuators in a thin cavity (0.5 mm thick) at the tip. The plasma discharges were obtained with steady operation, by applying a 1 kHz, 11 kV peak-to-peak sinusoidal voltage signal between the electrodes, using a 30/20A Trek amplifier. With such electrical parameters, the ionic wind maximal velocity is around 3 m/s as measured in Boucinha et al[17].

According to actuation effects obtained with the first eight arrangements and in view of reducing the main wing tip vortex strength, the second set of DBD arrangements was designed to reinforce action on the separation line of the primary vortex at the upper sharp edge, and on its attachment line located on the suction side. The tests consisted in firstly acting on each specific line, and secondly, on both lines simultaneously. A last test consisted in controlling the separation line at the lower sharp edge between the model pressure side and the marginal side as well. These control cases correspond to the arrangements presented in Fig. 6, DBD 9, DBD 3m (DBD 3 modified), and DBD 10 respectively. These DBD actuators consisted of two flush-mounted copper electrodes arranged asymmetrically on both sides of a dielectric composed of three 0.05-mm-thick polyimide layers. Actuators extended from 15% chord to 90% chord. For DBD9 and DBD3m actuators, the plasma discharges were obtained with steady actuation performed by applying a sinusoidal signal to the air-exposed electrode with a Minipuls 2 power supply delivering a high-voltage with a 24 kV peak-to-peak amplitude and a frequency of 8 kHz. For DBD 10 actuator, two power supplies were used: a 30/20 A Trek model power supply, for actuation on the separation lines, delivering a high-voltage with a 6.2 kV peak-to-peak amplitude and a frequency of 1.5 kHz, and the Minipuls 2, for actuation on the attachment line, with the same electrical parameters as above. During experiments, no large parametric study of operating electrical parameters was performed because of the numerous arrangements to be tested. The above parameters were mainly chosen in regard to previous experiments conducted with such actuators.

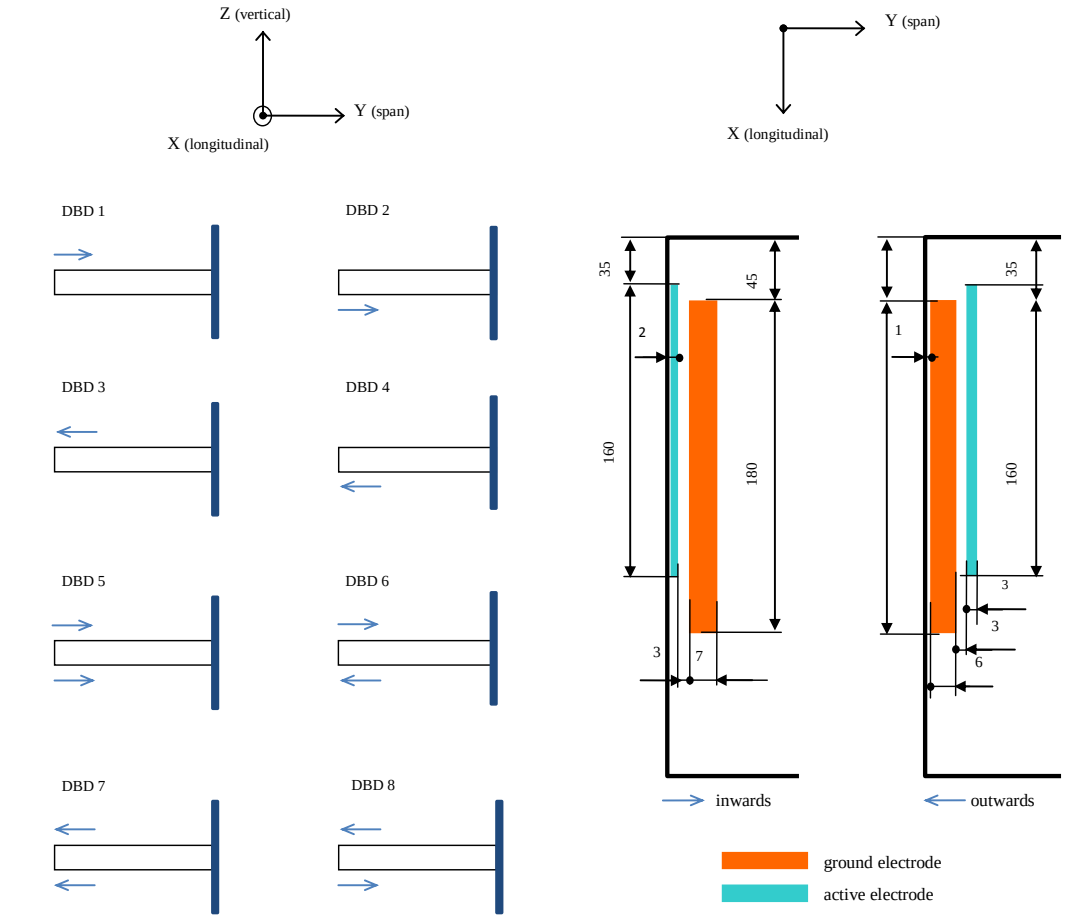

Figure 5. Schematic of the first set of DBD arrangements (dimensions in mm) and inward or outward direction of ionic wind (blue arrow).

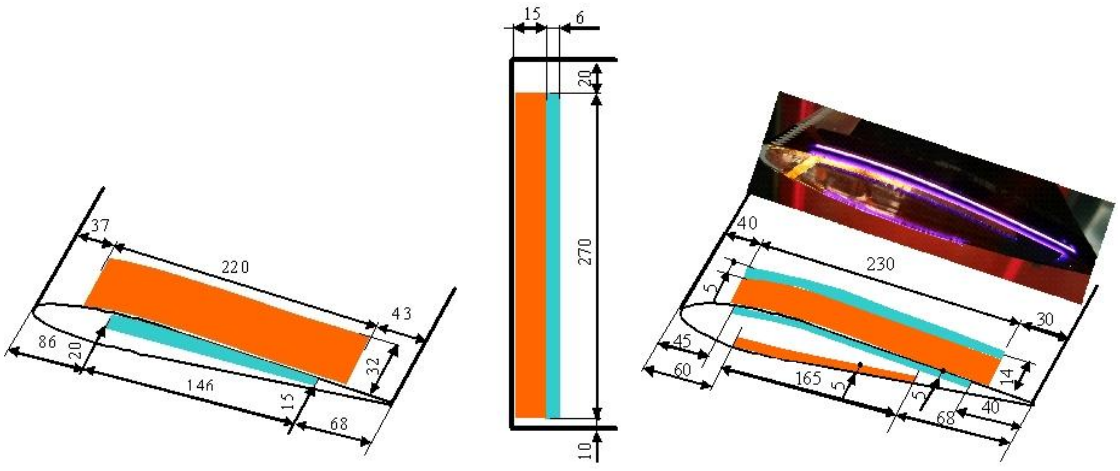

DBD 9 DBD 3m DBD 10

Figure 6: Schematic of the second set of DBD arrangements (dimensions in mm).

IV. Results and Discussions

The following results are presented for a freestream velocity of 10m/s and mainly concern the representation of the non-dimensional mean streamwise vorticity, transverse velocity, and turbulent kinetic energy (TKE) in the transverse planes shown in Fig. 3.

A. Effects of the first set of DBD arrangements

Figure 7 shows mean streamwise vorticity contours obtained with DBD 1. Baseline flow topology, corresponding to the case off in the plane X/c = -0.25 in Fig. 7, shows the separating shear layer which is detached at the upper sharp edge and forms the main primary vortex. The presence of a secondary vortex which rotates in the opposite direction can also be noted. Velocity fluctuations are concentrated in the shear layer, in the vortex core, and at the detachment line of the secondary vortex. Downstream in the plane X/c = 0.5, the main wake vortex is formed. When actuator is on, it can be observed in the plane X/c = -0.25 that the ionic wind interacts with the separation layer and with the secondary vortex, leading to its displacement and vertical extension as well as a decrease of its streamwise vorticity. Consequently the same effects on the primary vortex can be observed, namely a small displacement and a vorticity decrease of 20% in its core. Downstream in the plane X/c = 0.5, significant diffusion of the streamwise vorticity can be noted in the vortex core. Figure 8 shows mean streamwise vorticity contours obtained with DBD 3. When actuator is on, the ionic wind interacts with the secondary vortex by reducing its vorticity and its size. Thus, an enhancement of the primary vortex is here characterized by an increase of 15% in vorticity in the plane X/c = -0.25 and downstream in the plane X/c = 0.5 as well. Figure 9 shows mean streamwise vorticity contours obtained with DBD 4. When actuator is on, no significant modification of the main primary vortex is observable in the plane X/c = -0.25, even if vorticity is still slightly increased in the vicinity of the upper sharp edge.

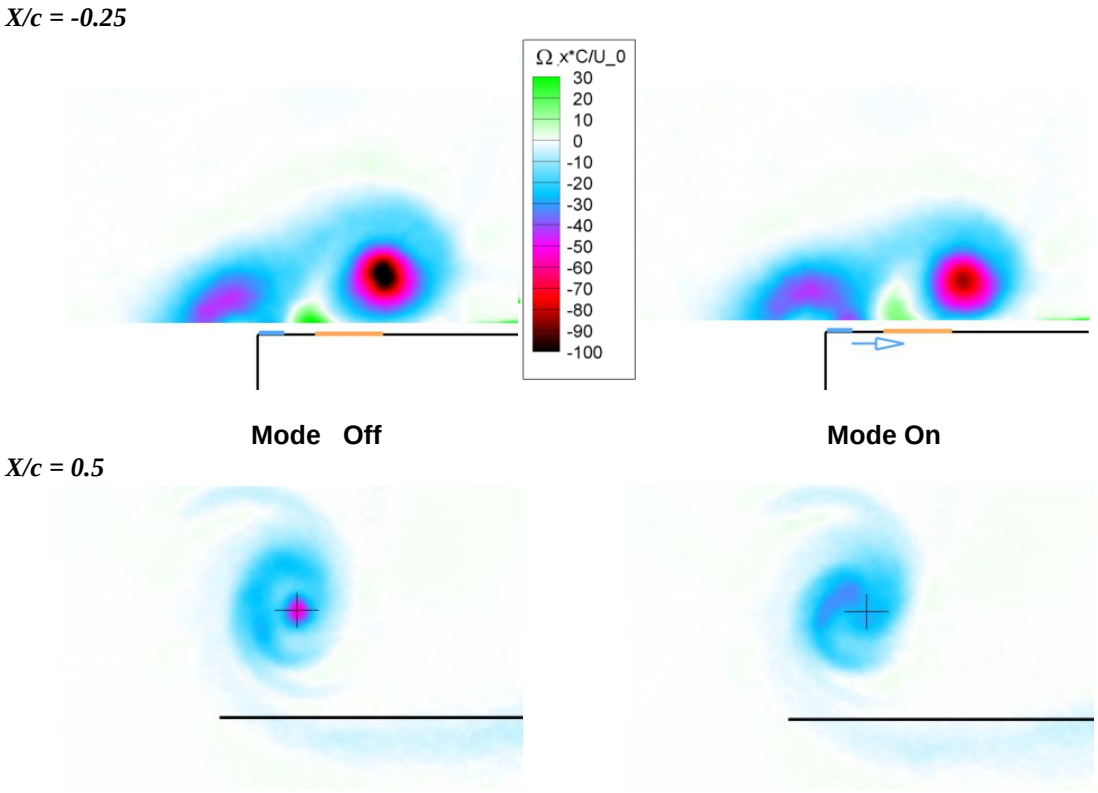

Figure 7. DBD 1, mean streamwise vorticity at X/c = -0.25 and X/c = 0.5, Off and On.

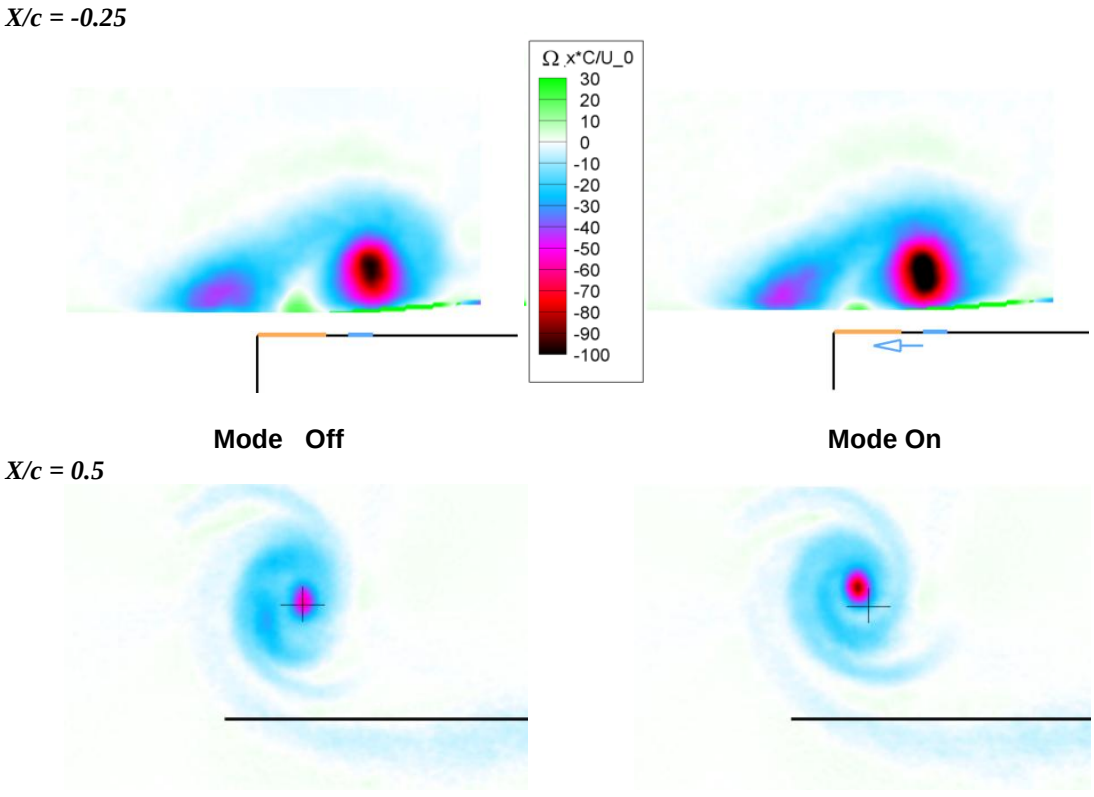

Figure 8. DBD 3, mean streamwise vorticity at X/c = -0.25 and X/c = 0.5, Off and On.

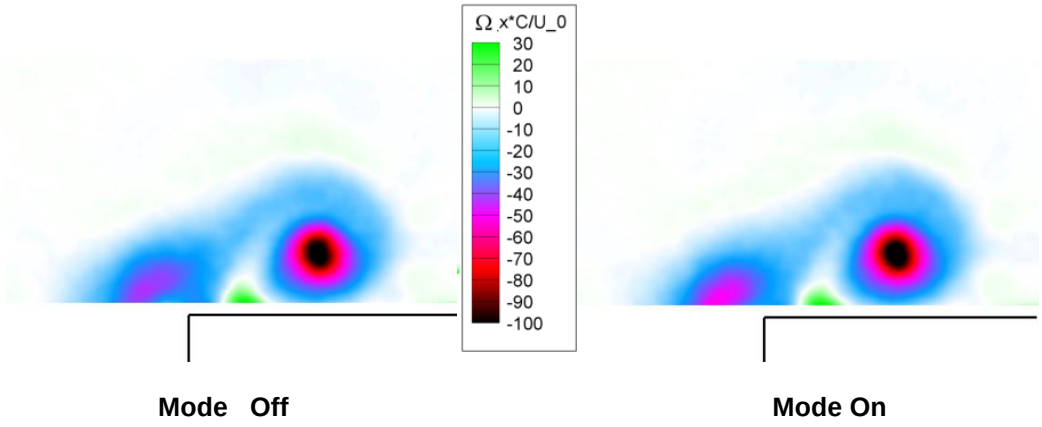

Figure 9. DBD 4, mean streamwise vorticity at X/c = -0.25, Off and On.

By comparing mean streamwise vorticity contours for each DBD arrangement presented in Fig. 5, it was finally observed that the most visible modification of the tip vortex was achieved with DBD 1 and 3 arrangements by operating one single DBD, and with DBD 6 and 7 arrangements by operating two DBDs simultaneously. Actually, for each arrangement and for the same electric power input, actuation in the pressure side was not as efficient as actuation in the suction side. It may be due to the fact that the induced flow by DBD actuators was insufficient in the operating conditions. Nevertheless it was with the inward flow arrangement that mean streamwise vorticity decrease was achieved in the main vortex core, the outward flow arrangement reinforcing it.

B. Effects of the second set of DBD arrangements

Figures 10-12 show transverse velocity, streamwise vorticity and TKE contours obtained with DBD 9. Activation of control manifests itself in the model by changing the orientation of the separating shear layers, a decrease of the velocity transverse component near the wall of the model as shown in Fig. 10, a change in the core location of the secondary vortex. These results denote a significant reduction in the formation of the vortex system. Thus, we note the decrease of the streamwise vorticity in Fig. 11, and an increase and a concentration of the TKE near the wing surface in Fig. 12. The effects of control persist downstream. Indeed a spatial shift of the vortex core can be observed, as well as vorticity diffusion of the order of 30%, and a reduction of TKE of about 25%.

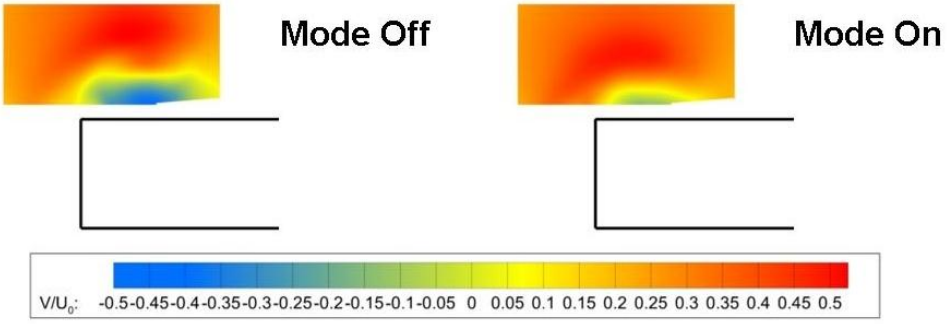

Figure 10. DBD 9, transverse velocity contours at X/c = -0.25, Off and On.

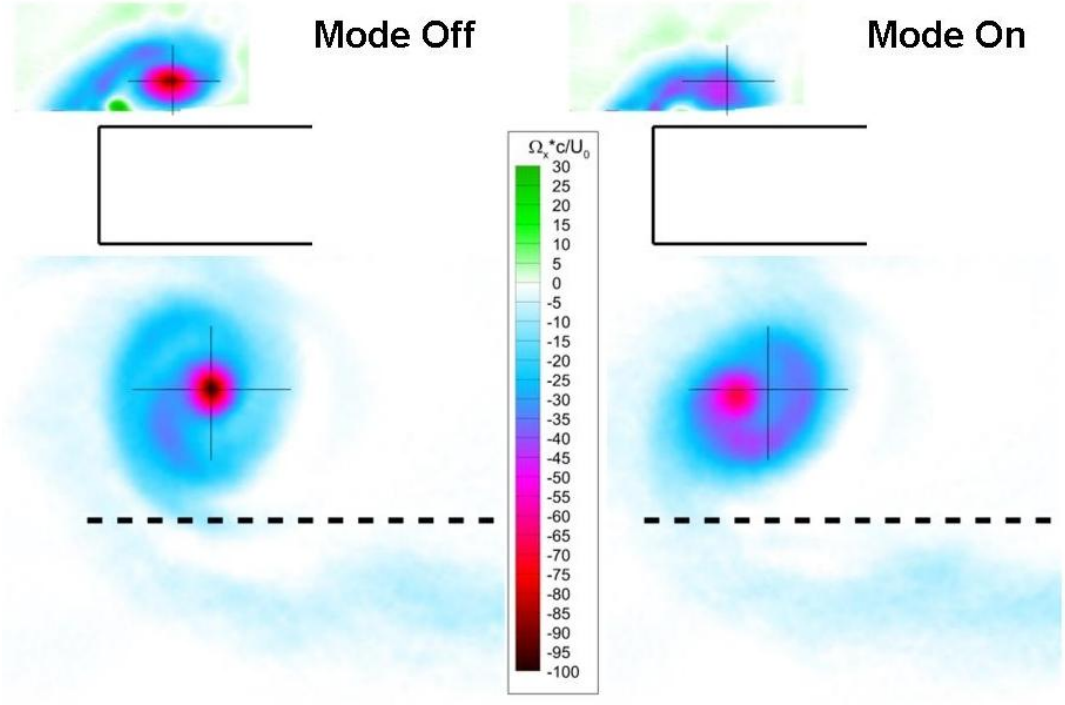

Figure 11. DBD 9, mean streamwise vorticity at X/c = -0.25 and X/c = 0.5, Off and On.

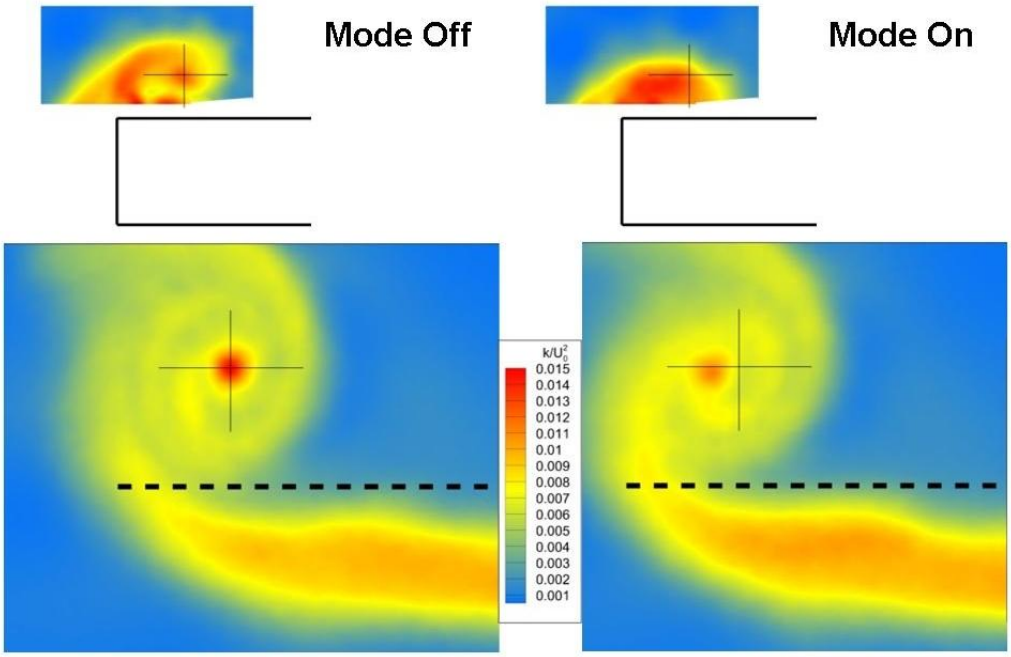

Figure 12. DBD 9, turbulent kinetic energy at X/c = -0.25 and X/c = 0.5, Off and On.

Figures 13-14 show streamwise vorticity and TKE contours obtained with DBD 3m (DB3 modified). The results have shown that the DBD 3 control increases the streamwise vorticity on the vortex core, due to its position in regard to the attachment line of the primary vortex. The DBD3m was then positioned so as to increase the transverse velocity at the attachment line of the main primary vortex even if the electrode position did not comply with the development of the conical main vortex. Indeed, DBD3m is effective only from X/c = -0.5. Results in the plane X/c = -0.25 show an increase of the transverse velocity component near the wall of the model, which results in a decrease of the streamwise vorticity in the primary vortex core as shown in Fig. 13, and a space reduction for the secondary vortex. TKE results in Fig. 14 show a reduction of fluctuations in the core of the primary vortex. This can be related to a stabilization of the vortex flow. Downstream in the plane X/c = 0.5 (not presented), weak effects of the actuator are absorbed by the main wake vortex without changing its characteristics significantly.

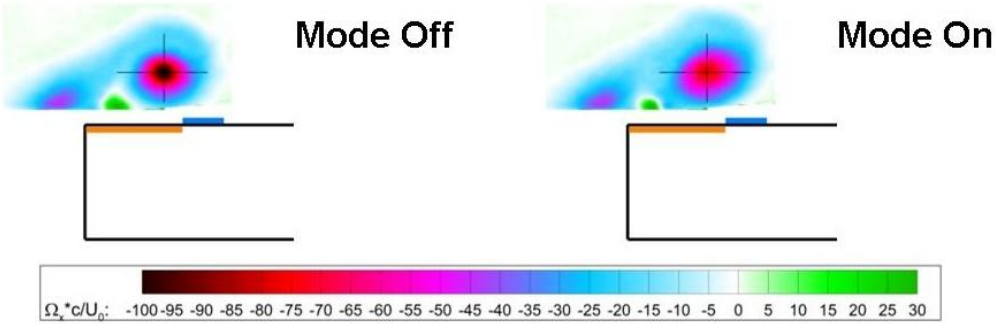

Figure 13. DBD 3m, mean streamwise vorticity at X/c = -0.25, Off and On.

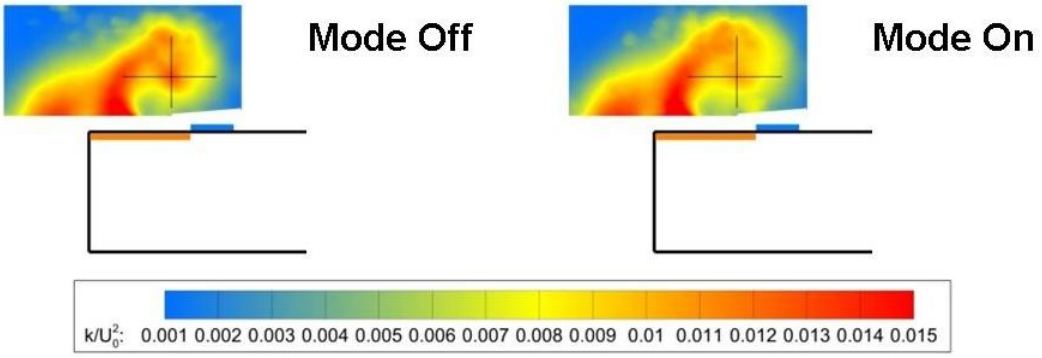

Figure 14. DBD 3m, turbulent kinetic energy at X/c = -0.25, Off and On.

Figures 15-16 show streamwise vorticity and TKE contours obtained with DBD 10. With actuators on, the ionic wind at the edge of the model interacts with the separating shear layer, characterized by a change of the mixed layer angle of incidence, and a reduction of the lateral space available for the secondary vortex. The ionic wind on the pressure side changes the flow below the main vortex and exerts attraction near the model wall (small vertical displacement of the vortex core). There is no change in the streamwise vorticity for the secondary vortex, whereas for the primary vortex it is decreased. Downstream, it can be observed a vertical displacement of the main wake vortex and a reduction of its streamwise vorticity.

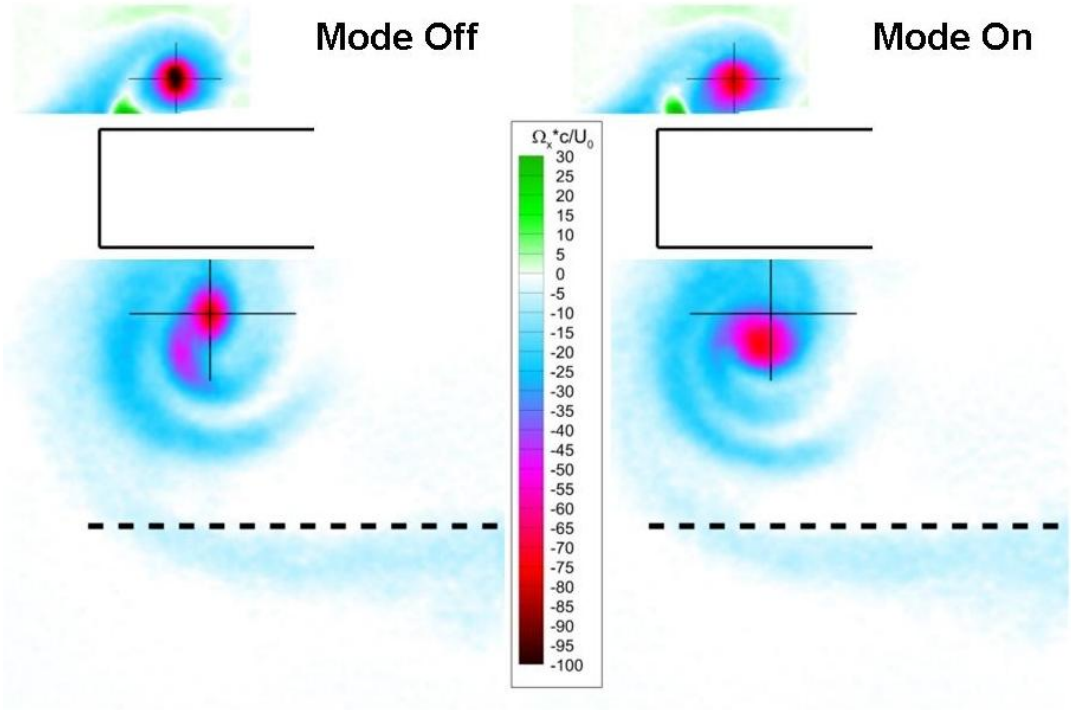

Figure 15. DBD 10, mean streamwise vorticity at X/c = -0.25 and X/c = 0.5, Off and On.

For the plane X/c = -0.25 in Fig. 16, TKE contours show, in the control case, an increase of flow instabilities on the separating shear layers and in the main vortex core. Downstream in the plane X/c = 0.5, the results show a reduction of the TKE level and a diffusion of the main vortex core.

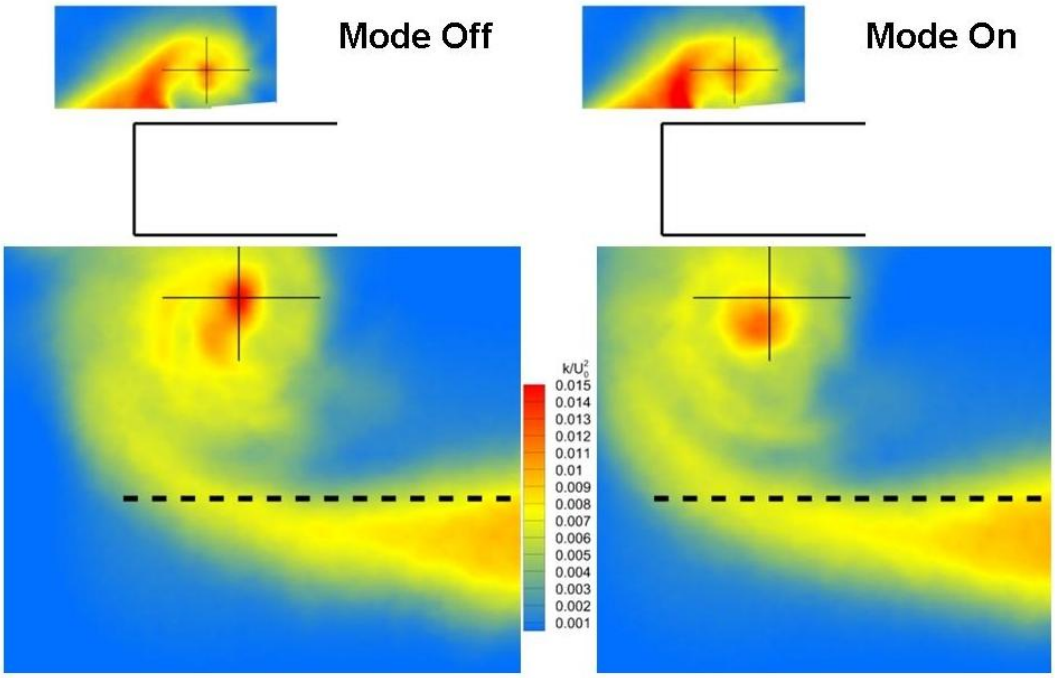

Figure 16. DBD 10, turbulent kinetic energy at X/c = -0.25 and X/c = 0.5, Off and On.

These results show modifications in the vortex system. Control changes the separating shear layers, including the vortex system generated between the pressure side and the end of the tip. Downstream in the plane X/c = 0.5, modifications result in a displacement of the vortex system and a diffusion of the main vortex core. However the combination DBD 9+DBD 3m is less effective than the control obtained only with DBD 9. The main assumption is that the ionic wind generated by the DBD 9 interacts with the one generated by the DBD 3m. The two ionic wind flows act in an area of small dimensions, and their opposite action limits the control beneficial effects.

C. Influence of the freestream velocity

Actuator influence on the flow field was examined for higher free stream velocities. On the model (X/c = -0.25) the flattening of the vortex system on the wing appears lower as the flow velocity increases (Fig. 17). Control no longer modifies the secondary vortex. However a displacement of the main wake vortex and a reduction of its streamwise vorticity are still observable. The increase of the freestream velocity stabilizes the main vortex. Indeed, TKE, plotted in Fig. 18, is only very slightly modified by the control. Downstream control actions persist. In the plane X/c = 0.5, results show a shift of the main wake vortex, a reduction of its streamwise vorticity of about 45% and a TKE reduction of about 25% as shown in Fig. 18. Finally, results have shown that actuator authority decreases while the free stream velocity increases higher than 25 m/s with operating electrical parameters given in section III.

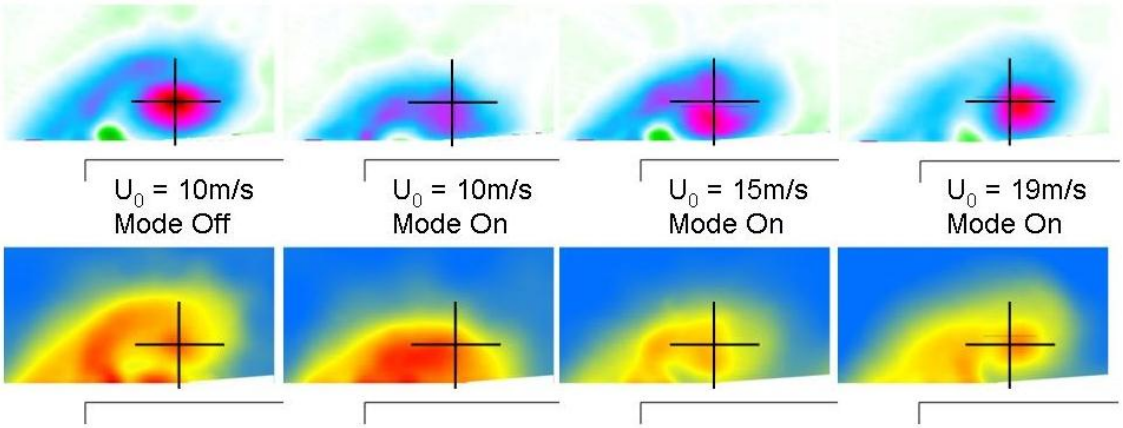

Figure 17. DBD 9, mean streamwise vorticity and turbulent kinetic energy at X/c = -0.25, Off and On. Freestream velocities U_0 = 10, 15 and 19 m/s.

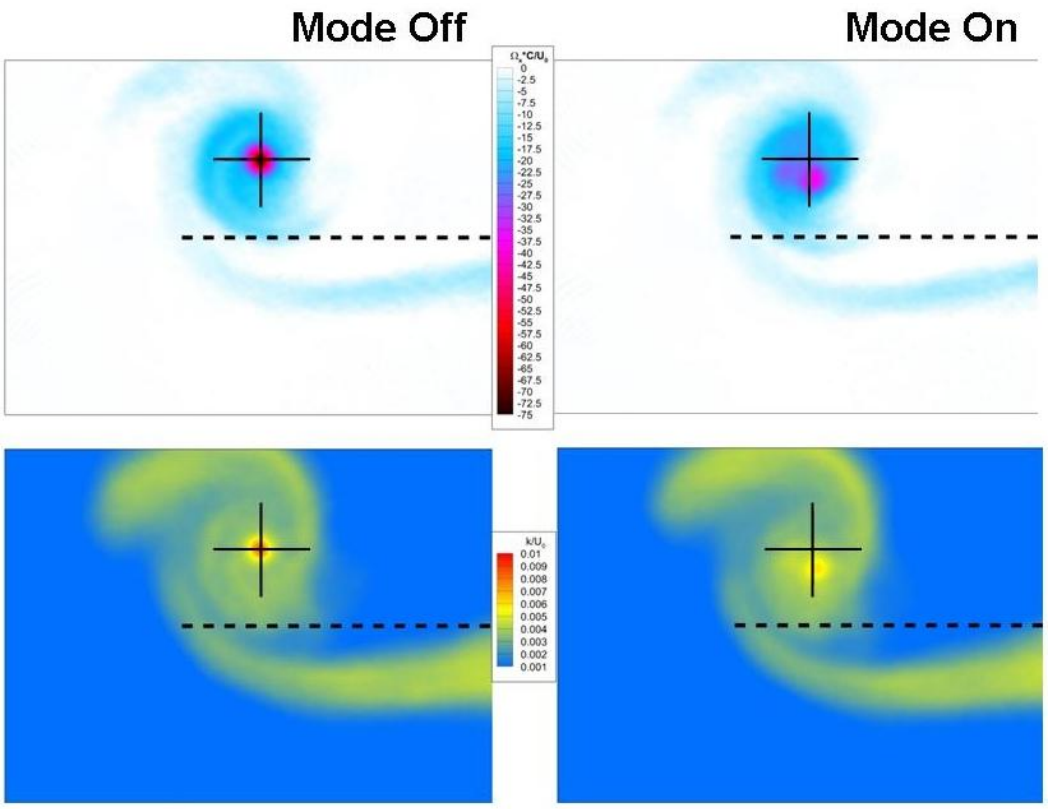

Figure 18. DBD 9, mean streamwise vorticity and turbulent kinetic energy at X/c = 0.5, Off and On. Freestream velocity U_0 = 19 m/s.

V. Conclusions

Effects of surface plasma actuation on the wing tip vortex characteristics, size and strength, were experimentally investigated by stereoscopic PIV. Different DBD arrangements near the wing tip were tested to examine and better understand effects of momentum addition on the formation and development of the vortex system emitted at the straight tip of a rectangular wing.

The results obtained during the tests show that effects of actuation mainly result in a local diffusion of the main wake vortex core and its displacement. It was established that the most effective reduction of vorticity was achieved by acting with inward flow arrangement on the separation line of the main primary vortex emitted on the wing. Finally, as for common applications of leading edge or trailing edge flow separation control by DBD actuators, the location of the DBD actuator remains a key parameter for optimizing control effects, as well as operating electrical parameters (frequency, amplitude, burst modulation of the high voltage for example).

Circulation calculation around the whole wake vortex in the plane X/c = 0.5 have been performed and did not yet show significant differences with and without actuation. Aerodynamic load measurements were not available for these tests. Consequently it was not possible to precisely quantify benefits of plasma actuation in terms of aerodynamic performances, such as lift increase or drag reduction for example. Nevertheless it has been demonstrated capabilities of surface DBD actuators to modify the wing tip vortex in order to reduce its strength. Further refined analysis of these results in regard to the literature concerning wing tip vortex control by passive and active devices is needed to estimate a real efficiency of this control.

Acknowledgments

The research leading to these results has received funding from the European Community's Seventh Framework Program FP7/2007-2013 under grant agreement n°234201.

The authors are greatly indebted to the F2 Wind Tunnel Group of the ONERA Fauga-Mauzac wind tunnel for performing the experiments.

At the University of Orleans, this work was performed in the framework of research federation EPEE* and of a collaboration with GREMI** for DBD actuator development.

*EPEE (FR0776 CNRS/University of Orleans)

**GREMI (UMR7344 CNRS/University of Orleans)

References

[1]Margaris P., Gursul I., "Effect of Steady Blowing on Wing Tip Flowfield", *2nd AIAA Flow Control Conference*, 28 June - 1 July 2004, Portland, USA, paper n°2004-2619.

[2]Brooks T.F., Marcolini, M.A., "Airfoil Tip Vortex Formation Noise", *AIAA Journal*, Vol. 24, N°2, 1986, pp. 246-252.

[3]Hui Li, Burggraf, O.R., Conslisk, A.T., "Formation of a Rotor Tip Vortex", *Journal of Aircraft*, Vol. 39, N°5, pp. 739-749, September-October2002.

[4]Cousin, D., Morikone, M., Hirst, S., Elder, J., Ilie, M., "Experimental studies of tip-vortex formation; influence of blade-tip geometry on the vortex characteristics*", 49th AIAA Aerospace Sciences and Meeting including The New Horizons Forum and Aerospace Exposition*, 4 - 7 January 2011, Orlando, Florida, paper n°2011-1253.

[5]M. Mitchell, A., Délery, J., "Research into vortex breakdown control", *Progress in Aerospace Sciences*, Vol. 37, 2001, pp. 385-418.

[6]Ramaprian, B.R., Zheng, Y., "Measurements in Rollup region of the Tip Vortex from a Rectangular Wing", *AIAA Journal*, Vol. 35, N°12, 1997, pp. 1837-1843.

[7]Corke, T.C., Enloe, C.L., Wilkinson, S.P., "Dielectric barrier discharge plasma actuators for flow control", *Annual Review in Fluid Mechanics*, Vol. 42, pp. 505–529, 2010.

[8]Budovsky A.D., Sidorenko, A.A., Maslov, A.A., Zanin, B.Y., Zverkov, I.D., Postnikov, B.V., Kozlov, V.V., "Plasma Control Of Vortex Flow On Delta-Wing At High Angles Of Attack", *47th AIAA Aerospace Sciences Meeting Including The New Horizons Forum and Aerospace Exposition*, 5 - 8 January 2009, Orlando, Florida, paper n°2009-888.

[9]Boesch, G., Vo, H.D., Savard, B., Wanko-Tchatchouang, C., Mureithi, N.W., "Flight Control Using Wing-Tip Plasma Actuation", *Journal of Aircraft*, Vol. 47, No. 6, 2010.

[10]Hasebe, H., Naka, Y., Fukagata, K., "An Attempt for Suppression of Wing-Tip Vortex Using Plasma Actuators", *Journal of Fluid Science and Technology*, Vol. 6, No. 6, 2011.

[11]Agibalova, S. A., Golub, V. V., Moralev, I. A., and Saveliev, A. S., "Effect of Dielectric Barrier Discharge on Wing Tip Vortex Formation", *Technical Physics Letters*, Vol. 37, No. 11, pp. 1070–1073, 2011.

[12]Birch, D., Lee, T., Mokhtarian, F. and Kafyeke, F., "Rollup and Near-Field Behavior of a Tip Vortex", *Journal of Aircraft*, Vol. 40, N° 3, engineering notes, 2003.

[13]Ghias, R., Mittal, R., Dong, H., S. Lund, T., "Study of Tip-Vortex Formation Using Large-Eddy Simulation", 43th Fluid Dynamics Conference and Exhibit AIAA, 10-13th January 2005, Reno, USA, paper n°2005-1280.

[14]Margaris, P., Gursul, I.," Vortex topology of wing tip blowing", Aerospace Science and Technology, Vol. 14, 2010, pp. 143–160.

[15]Leclaire, B., Jaubert, B., Champagnat, F., Le Besnerais, G., Le Sant, Y.,"FOLKI-3C: a sample, fats and direct algorithm for stereo PIV", *Proceedings 8th International Symposium on PIV - PIV09*, Melbourne, Victoria, Australia, August 25-28, 2009.

[16] Champagnat, F., Plyer, A., Le Besnerais, G., Leclaire, B., and Le Sant, Y., "How to Calculate Dense PIV Vector Fields at Video Rates", *Proceedings of 8th International Symposium on Particle Image Velocimetry - PIV09*, Melbourne, Australia, August 25-28, 2009.

[17] Boucinha, V., Magnier, P., Leroy, A., Weber, R., Dong B., Hong, D., "Characterization of the Ionic Wind Induced by a Sine DBD Actuator used for Laminar-to-Turbulent Transition Delay by LDV", *4th AIAA Flow Control Conference*, Seattle, 23-26th June 2008, paper N°2008-4210.